Kemal Yaman ✉
M. Burak Dalmış

https://doi.org/10.21278/TOF.502080725
ISSN 1333-1124
eISSN 1849-1391

INFLUENCE OF UNDER-WING STORE MASS ON THE FLUTTER RESPONSE OF AN F-16 MODEL WING

Summary

This study investigates the effect of tip-mounted store mass on the flutter behaviour of an F-16 fighter jet model wing using wind tunnel testing and numerical analysis. A 1/8-scale polycarbonate wing was tested with six external store configurations of identical geometry but different masses, representing varying inertia through aluminium and steel materials. Experiments were conducted in the Ankara Wind Tunnel, while numerical analyses were performed in ZAERO® using modal data obtained from finite-element models. Seven configurations, including a clean wing baseline, were evaluated with stores mounted on F-16 under-wing stations. A comparison of ZAERO's g-method and k-method showed that the k-method exhibits closer agreement with experimental results. The findings reveal that increasing store mass leads to a pronounced reduction in flutter frequency and flutter speed, and this trend becomes increasingly non-linear for heavier configurations. These results underscore the dominant role of tip-mounted inertia in subsonic flutter behaviour and demonstrate that simplified flat-plate wing models can reliably capture mass-driven aeroelastic trends.

Key words: flutter; modal analysis; plate vibration; subsonic flow; wind tunnel; wing store

1. Introduction

Commercial aircraft, military jets, and unmanned aerial vehicles often carry various types of external stores, which are not deployed arbitrarily but within an operational framework. This framework defines the type, number, and placement of stores on the aircraft. The mass and location of the store, moments of inertia, and centre of gravity significantly influence natural frequencies, mode shapes and ultimately, flutter speed and frequency. Each external configuration possesses unique structural and aerodynamic properties, requiring tailored certification testing procedures for flutter assessment. Such tests play a crucial role in aircraft design and modification. Flutter research began with investigations by Lanchester [1] and Bairstow and Fage [2] into asymmetric flutter on the Handley Page bomber in 1916. Blasius [3] later examined performance deficiencies in the Albatros D3 biplane. Torsional flutter was later expanded upon by Smilg [4]. Single degree-of-freedom flutter modes were observed on control surfaces at subsonic and supersonic speeds [5]. Wings heavier than the surrounding air with significant sweep angles may experience pure bending flutter [6]. Greidanus [7] studied bending-torsion under incompressible flow, while Dugundji [8] and Dowell [9] focused on panel flutter and nonlinear plate oscillations. Kosmatka [10] applied a force-series solution for cantilever beams with tip masses.

Studies on the influence of store mass on flutter under subsonic flow remain relatively limited compared to transonic research. Turner [11] analysed 308 configurations and found that flutter initiates aeroelastic instability but is generally unaffected by store aerodynamics. Fazelzadeh et al. [12] evaluated equivalent mass distributions in different positions and reported that store mass reduces flutter speed. Farhat et al. [13] modelled fuel sloshing effects and noted a proportional decrease in flutter speed with fuel consumption at 0.5 Mach, with more severe reductions near transonic speeds. Jun [14] compared clean wings with missile-tip configurations and showed a drop in flutter speed from 650 to 460 knots depending on mass and aerodynamic effects. Janardhan and Grandhi [15] studied how store parameters influence flutter and limit cycle oscillations (LCO). Even under small disturbances, aerodynamic and structural coupling creates complex nonlinear behaviour, particularly in transonic flow where shock waves and wing geometry amplify the system's response. Librescu and Song [16] further noted that wing-tip stores reduce flutter frequency more than underwing loads.

Recent works, including Currao [17], demonstrated stall-induced flutter modes through combined numerical and experimental studies on thin plates. Goizueta et al. [18] analysed flexible wings using SHARPy and MRM reduced-order models and showed that wing deformation can shift flutter boundaries. In modern fighters, strong coupling between structural dynamics and flight control systems has motivated aeroservoelastic studies, showing that feedback can shift flutter margins and stability boundaries [19]. Related work has examined advanced control concepts, including multi-input/output architectures and nonlinear dynamic inversion, as practical means to improve aeroelastic robustness in high-performance configurations [20]. Healy et al. [21] investigated floating wingtip fuel tanks and reported that fuel motion alters dynamic loads and aeroelastic response. Yu et al. [22] examined wing-pylon-nacelle configurations in subsonic and supersonic regimes using continuation methods and reported improved accuracy over classical p-k methods. Basiri [23] and Balakrishnan [24] showed that equivalent plate models with Doublet Point methods capture key flutter trends for low-aspect-ratio delta wings. Clean wing studies [25] have emphasised wind tunnel validation for local flow effects, while scaled composite experiments require careful aeroelastic similarity criteria [26]. Dinulovic et al. [27] applied machine learning to predict flutter of composite missile fins, indicating promise for early-stage assessment. However, whereas these studies mainly address aerodynamic complexity, control interaction, or material effects, the present work isolates external-store mass by testing and simulating geometrically identical stores with different inertial properties on an F-16 model wing.

External stores can reshape fighter-wing aeroelastic stability; changes in mass, inertia, and station location may shift flutter onset and trigger or suppress LCO. Chen et al. [28] reported these effects for an F-16 with external stores, while Lee and Chen [29] analysed the aerodynamic influence of under-wing stores in the transonic regime. The present simulations use ZAERO following the theoretical formulation and flutter-module procedures of ZONA Technology Inc. [30]. Experimental wing–store correlation studies (including nonlinear response) have been demonstrated by Tang and Dowell [31], and the broader implications of store loading on advanced wings were discussed by Gern and Librescu [32]. Most importantly, Yaman [33] provided a directly relevant baseline by validating ZAERO (including the g-method) against wind tunnel data for a cantilever plate-type wing, which underpins the verification strategy adopted here. The damping-perturbation g-method that ZAERO builds on was formulated by Chen [34]. For F-16 practice, Pollock et al. [35] evaluated flutter prediction for store-equipped configurations, while Bennani et al. [36] examined heavy-store cases using robust analysis strategies. Santos et al. [37] detailed how external-store aerodynamics should be represented in subsonic flutter assessments, and Maxwell et al. [38] provided a ZAERO/ZONA-based implementation perspective for incorporating store-aerodynamic effects. Robust treatment of uncertain store aerodynamics was addressed by Heinze et al. [39], while Cui and Han [40] examined tip/appendage effects. Golparvar et al. [41] measured related trends through nonlinear experiments. Pylon nonlinearities were investigated by Gilioli et al. [42], and numerical stabilisation techniques were developed by Yuan and Zhang [43]. Efficient

LCO prediction strategies were reported by Kariv et al. [44]. Finally, model updating via ground vibration testing supports certification-grade flutter prediction and correlation [45].

In this study, the required modal inputs were generated using MSC NASTRAN®, and structural models were created in MSC PATRAN®. All flutter tests were validated through wind tunnel experiments at the Ankara Wind Tunnel (ART). The novelty of this study lies in experimentally isolating the mass effect by analysing aluminium and steel stores with identical geometry and evaluating configurations where store mass significantly exceeds the wing's own weight.

2. Methodology

Within the scope of this study, a structure resembling the F-16 wing was analysed and tested in terms of flutter behaviour. The F-16 fighter aircraft, due to its broad mission profile and widespread operational use, serves as an ideal platform for examining external store interactions. For the wind tunnel tests, a 5 mm thick polycarbonate (PC) plate with an F-16 wing (trapezoidal) shape was employed. This plate allowed the mounting of external stores for flutter evaluation. During the tests, six different cylindrical stores with a 45° chamfered tip were used as wing-tip loads. The stores were mounted on either the second or eighth underwing station (Fig. 1), consistent with the actual F-16 configuration. Due to geometric constraints, the corresponding pylon structure was not included in the test setup. The configurations of these pencil-shaped stores are presented in Table 1.

Fig. 1 Underwing store configurations of F-16 fighter jet

Table 1 Store configuration employed on the 1/8 Scale F-16 wing plate

Store no	Material type	Diameter (mm)	Length (mm)	Weight (g)
1	Aluminium	10	363	70
2	Aluminium	20	363	300
3	Aluminium	40	363	1200
4	Steel	10	363	224
5	Steel	20	363	894
6	Steel	40	363	3576

As also noted by Turner [11], many studies on flutter analysis involving external stores tend to neglect their aerodynamic characteristics. This is primarily because aerodynamic effects are often considered secondary, and accounting for them significantly increases the complexity and computational effort required for flutter analysis. For this reason, a simple cylindrical pencil-shaped store geometry was adopted in the present study. Figure 2 illustrates the experimental setup of the PC wing-plate structure and its configuration in the Ankara Wind Tunnel (ART). The PC plate was positioned parallel to the airflow during testing.

The experiments were conducted in the low-speed test section of the Ankara Wind Tunnel (ART), which has a 1.95 m × 1.95 m cross-section and a test length of 2.5 m. The tunnel operates in the velocity range of 10–110 m/s, corresponding to Mach numbers between 0.03 and 0.30, and Reynolds numbers in the order of 10^5–10^6 ($\approx 2.3\text{x}10^5$) based on the model chord length. All tests were performed at zero angle of attack.

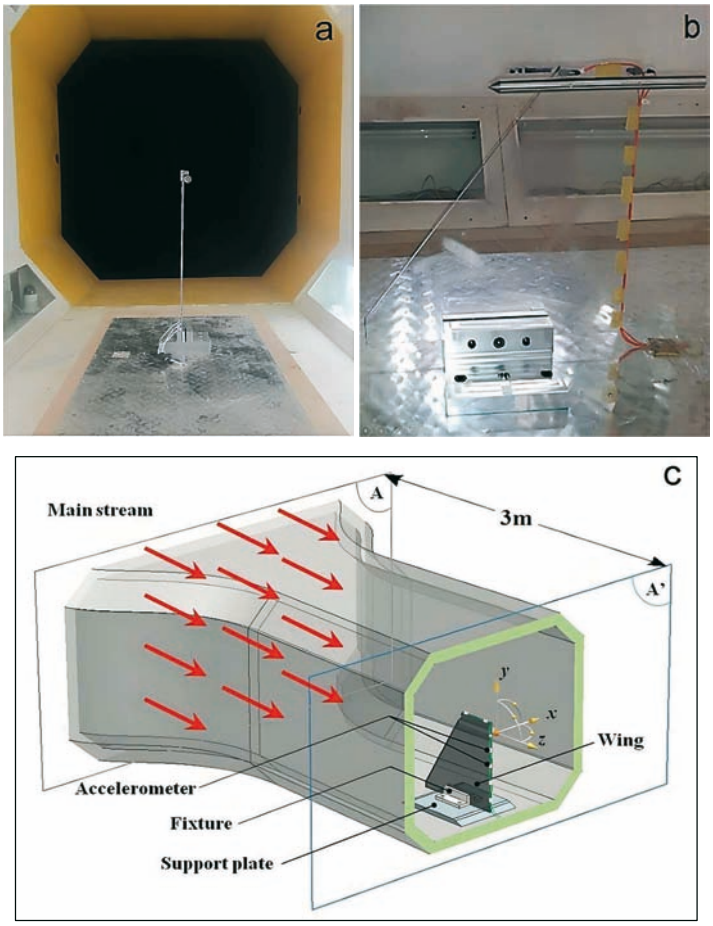

Fig. 2 Experimental setup for wing with tip-store: (a) ART, (b) setup, (c) schematic of wind tunnel A-A' section

As shown in Fig. 2b, the plate was rigidly mounted to the tunnel floor using a custom-designed fixture. To collect strain data, tri-axial strain gauges manufactured by Vishay were applied to the root section of the plate. For acceleration measurements, Brüel-Kjær accelerometers, models 4507B and 4508B, were employed. Data acquisition was carried out using an NI 9234 data acquisition system, and the recorded signals were processed using the LabView® software platform. The mechanical properties of the polycarbonate (PC) material used in the finite element model of the wing plate structure are listed in Table 2. The values for Young's modulus, Poisson's ratio, and material density were adopted from Yaman's previous study [33].

The aeroelastic model of the wing plate is discretised into 20 elements along the x-axis and 17 elements along the y-axis. For the munition body, the model includes 25 elements in the y-direction. The finite element model was constructed using Patran and subsequently analysed using Nastran. In these analyses, Nastran's standard modal analysis module was used and quadrilateral shell elements (Quad elements) were preferred in the prepared models.

Table 2 PC Material properties

Property	**Value**
Elastic modulus [GPa]	2.25
Poisson ratio	0.35
Density [kg/m^3]	1200
Mass [kg]	**0.754**
I_x [kg.m^2]	1.127134
I_y [kg.m^2]	0.716040
I_z [kg.m^2]	0.413483

Modal analyses or in situ vibration tests (GVT) of the plate structures were performed using MSC-Nastran finite element models. Finite element (FE) models were created for the F-16 wing plate. The trapezoidal wing plate has a root chord of 496 mm, a tip chord of 144 mm, and a semi-span of 418 mm. The boundary conditions and modal parameters with the best correlation with the modal test data were used in the flutter analyses. The nomenclatures and measurements of the finite element model are presented in Fig. 3. All tip-store models have a total length of 363 mm with a cylindrical mid-section and a 45° chamfered conical tip, as illustrated in the figure.

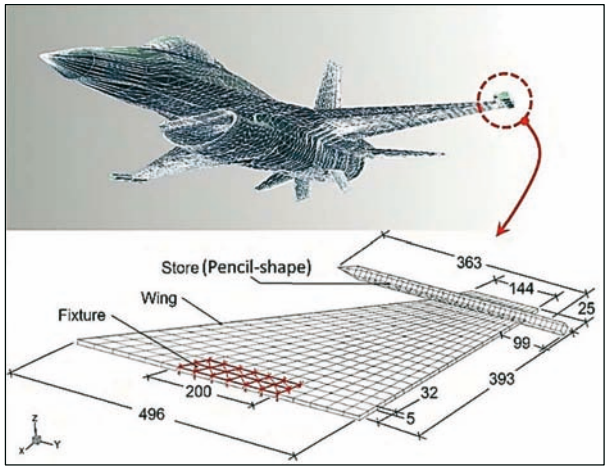

Fig. 3 FE model of F-16 wing (20×17 elements) with tip-store and root fixation dimensions

Ground Vibration Testing (GVT) is crucial for validating and refining an aircraft's mathematical model by using experimentally identified low-frequency mode shapes of the full structure. These mode shapes are used to verify the initial analytical model, and the GVT results are then used to update the finite element (FE) model. Once validated, the FE model can be used to predict critical flutter speeds, so the model-updating process must be performed carefully, as noted by Göge et al. [45]. In this study, natural frequencies were obtained via impact hammer modal testing to compare FE results with wind tunnel measurements. GVT can be performed using either a shaker or an impact hammer. In the shaker setup, accelerometer locations were defined on the wing plate (with additional sensors near the tips), accelerometers were installed, and boundary conditions were specified in MSPro®; however, the shaker test proved unreliable because the combined mass of sensors and actuators caused excessive wing deformation. Therefore, the impact hammer method was adopted: a similar instrumentation layout was used, manual excitation was applied at predetermined points, and the resulting data were more reliable. These measurements were then used to define FE boundary conditions, improving the accuracy of subsequent numerical analyses.

3. Results and Discussion

This section presents the set of analysis and test results obtained from various wing configurations, including the clean wing and wings equipped with aluminium and steel stores of 10, 20, and 40 mm in diameter. The methods covered comprise wind tunnel testing, finite element analysis, modal testing (commonly referred to as Ground Vibration Testing or GVT), and simulations performed using the ZAERO software. A comparative evaluation of the results is provided, followed by a discussion of the findings in relation to existing literature.

3.1 Wind tunnel test results

Wind tunnel testing was conducted for various combinations of 1/8 scale F-16 wing plates. As illustrated in Fig. 2b, the wing plate was mounted to the wind tunnel floor using a custom fixture. During the tests, acceleration data were collected through accelerometers. The

placement of these accelerometers is shown in Fig. 4. Figure 5 presents the acceleration responses obtained from four separate channels, along with the corresponding acceleration–time graphs and power spectral density (PSD) versus frequency plots.

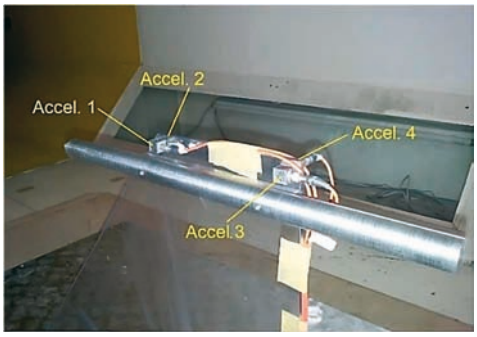

Fig. 4 Accelerometer placement for F-16 wing plate with store in wind tunnel

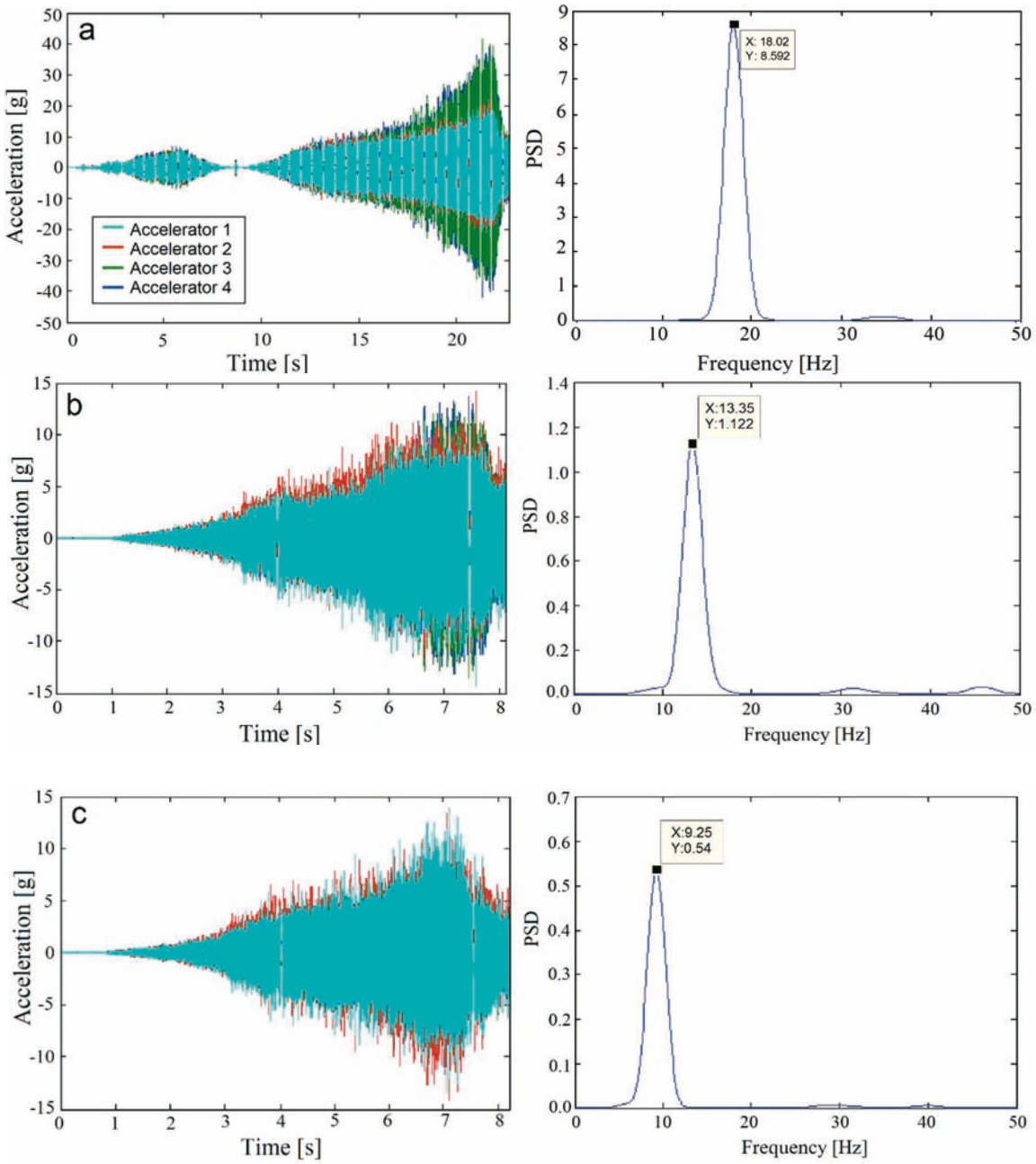

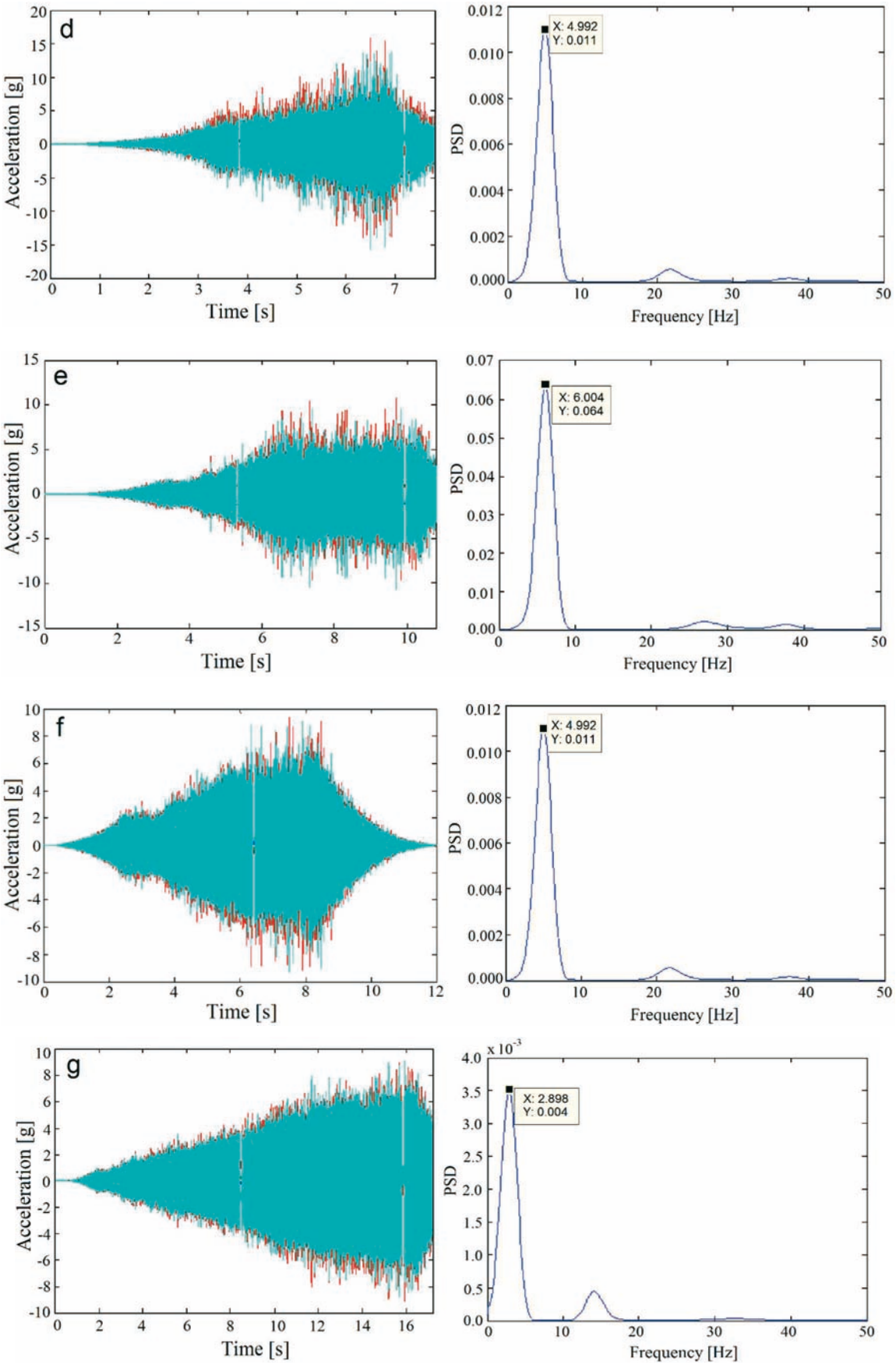

Fig. 5 Acceleration–time and PSD–frequency plots for (a) clean wing,
(b–d) aluminium stores (Ø10, Ø20, Ø40 mm), and (e–g) steel stores (Ø10, Ø20, Ø40 mm)

The acceleration–time and PSD–frequency graphs are presented in Fig. 5a for the clean wing and in Fig. 5g for the wing configuration carrying a 40 mm diameter steel store. These figures clearly demonstrate that during the onset of flutter, the acceleration signals rise sharply and uncontrollably, followed by a rapid decline once the wind tunnel is shut down. This behaviour consistently indicates the moment of flutter initiation and subsequent stabilisation. Post-processing of the recorded acceleration data allows for the identification of the dominant flutter frequency corresponding to each tested configuration. The resulting flutter frequencies are indicated explicitly on the right-hand side of Fig. 5a for the clean wing case and Fig. 5g for the configuration with the Ø40 mm steel store, respectively. A detailed summary of the wind tunnel test results for full-span plate configurations is provided in Table 3. A clear downward trend in flutter speed is observed as the mass of the store mounted on the plate increases, which aligns with general expectations based on added mass effects. However, this trend appears to break down in the case of the Ø40 mm steel store configuration. In this specific case, it is likely that excessive structural displacement of the plate introduced a stronger nonlinear response, which may have caused the flutter behaviour to deviate from typical patterns. As a result, an unexpected increase in flutter speed was observed, contrary to the trend seen in lighter configurations.

Table 3 Flutter results for wing-type plates in ART wind tunnel

Test #	Test configuration	Flutter speed (m/s)	Flutter freq. (Hz)
1	Clean wing	72.92	18.02
2	Wing with Ø10 mm aluminium store, (W= 70g)	69.97	13.35
3	Wing with Ø20 mm aluminium store, (W= 300g)	66.80	9.250
4	Wing with Ø40 mm aluminium store, (W= 1200g)	61.56	4.990
5	Wing with Ø10 mm steel store, (W= 224g)	67.63	10.55
6	Wing with Ø20 mm steel store, (W= 894g)	64.61	6.040
7	Wing with Ø40 mm steel store, (W= 3576g)	63.16	2.694

As the wing-tip mass increases, the flutter onset speeds exhibit an approximately linear decrease, as shown in Table 3. This reduction is slightly more pronounced for aluminium masses compared to steel masses of the same size. Flutter frequencies also show a decreasing trend with increasing mass. The highest flutter speed and frequency were obtained from the clean wing configuration, measured as 72.92 m/s and 18.02 Hz, respectively. In contrast, for the Ø40 mm steel store, these values were recorded as 63.16 m/s for speed and 2.940 Hz for frequency. As presented in the table, the decrease in flutter frequency becomes more significant than the corresponding reduction in flutter speed as the store mass increases. Although the simplified flat-plate configuration neglects detailed aerodynamic effects of a realistic airfoil, it provides a valid comparative basis for isolating the influence of store mass on flutter parameters.

3.2 FEA and GVT results of F-16 wing plate with and without external stores

Figure 6 displays the initial four natural frequencies and associated mode shapes of the F-16 clean wing plate (without store), considering a boundary condition in which the plate is fixed solely at its root. Similarly, Fig. 7 shows the corresponding vibrational characteristics for the F-16 wing plate equipped with a 40 mm diameter steel store at the tip, evaluated under the same root-fixed constraint.

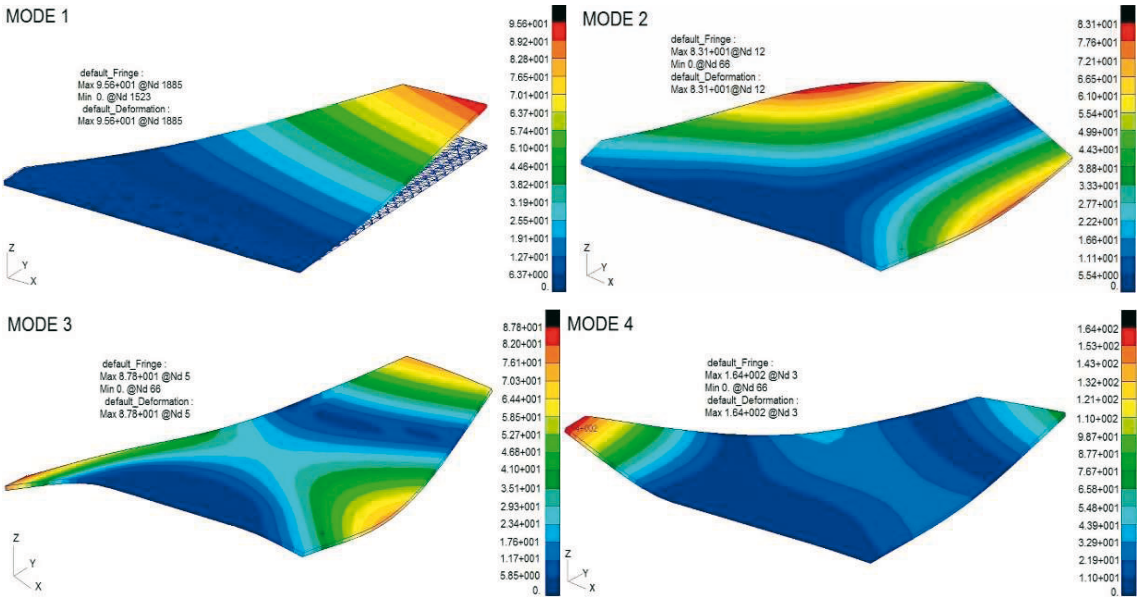

Fig. 6 First four natural frequencies and mode shapes for wing plate without store

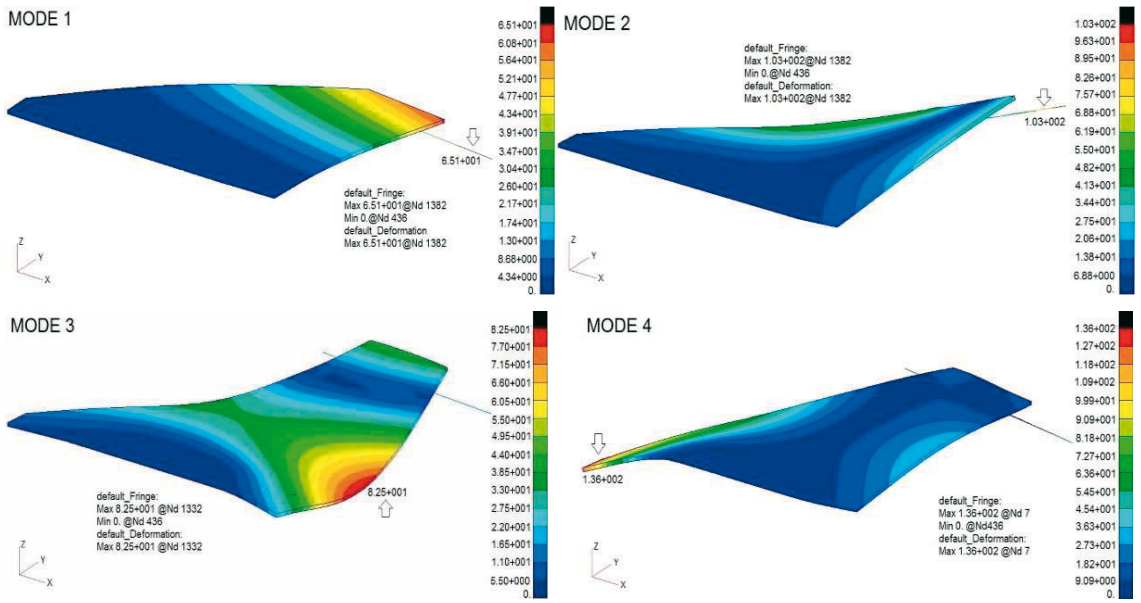

Fig. 7 First four natural frequencies and mode shapes for wing plate with Ø40 mm steel store

A mesh convergence study was carried out by refining the FE grid from 10×8 to 20×17 elements. Natural frequencies varied less than 1.5% beyond this mesh, indicating convergence. Aerodynamic loads in ZAERO were computed using the ZONA6 potential flow solver with doublet lattice-based unsteady aerodynamic influence coefficients.

When the maximum deformations are examined, much higher displacement values are obtained for the clean wing compared to the wing equipped with the Ø40 mm steel store. The under-wing store mounted at the tip reduces the natural frequency of the wing, causing it to vibrate at lower speeds. As a result, the maximum amplitudes observed at the natural frequency are slightly lower than those of the clean wing. These analyses show that as the outer store mass increases, the speed at which the wing reaches the vibration speed decreases. Pollock et al. [35] and Balakrishnan et al. [24] reported in their respective studies that each additional mass placed on the clean wing increases the force acting on the structure when the under-wing/wing-tip store is used and decreases the vibration speed compared to the clean configuration. For the ZAERO

flap analysis, the natural frequencies of both the clean and store-mounted wing configurations were determined according to the Ground Vibration Test (GVT) results.

The findings presented in Table 4 and Fig. 8 demonstrate that the results of Finite Element Method (FEM) analyses are in strong agreement with the GVT outcomes, confirming that natural frequencies can be accurately predicted through simulation. This alignment offers significant benefits to aircraft designers in terms of cost effectiveness and feasibility. Since GVT typically requires access to a physical aircraft, conducting such tests for fighter aircraft often involves substantial time allocation and bureaucratic procedures.

Table 4 Numerical (FEA) and experimental (Modal) first 4 frequencies of F-16 wing plate

Wing tip	**Clean wing**		**Ø10 mm al. store**		**Ø20 mm al. store**		**Ø40 mm al. store**		**Ø10 mm steel store**		**Ø20 mm steel store**		**Ø40 mm steel store**	
Mode number	Freq.(Hz) FEA	Freq.(Hz) modal test	Freq.(Hz) FEA	Freq. (Hz) modal test	Freq. (Hz) FEA	Freq. (Hz) modal test	Freq. (Hz) FEA	Freq. (Hz) modal test	Freq. (Hz) FEA	Freq. (Hz) modal test	Freq. (Hz) FEA	Freq. (Hz) modal test	Freq. (Hz) FEA	Freq. (Hz) modal test
1	7.10	7.06	5.47	5.34	3.94	3.94	2.15	2.28	4.36	4.38	2.60	2.68	1.37	1.29
2	22.7	24.8	14.8	18.9	10.9	12.4	6.20	6.72	12.1	14.4	7.15	8.10	3.76	4.07
3	34.6	33.6	29.3	30.1	25.3	27.7	21.3	20.5	26.2	29.0	23.2	25.2	20.7	14.5
4	51.0	57.8	35.5	46.2	33.4	41.1	31.7	39.2	33.9	42.3	32.4	47.9	31.7	25.9

Table 4 presents the first four natural frequencies of the finite element (FE) model for both the clean wing and the wing with an underwing-tip store, along with the corresponding results obtained from ground vibration (modal) testing. A comparison between the modal analysis and experimental results indicates that, across all external store configurations, the first mode frequencies derived from FE analysis align more closely with the test data (Fig. 8).

Consequently, it is expected that flutter analysis based on the first mode shapes would yield more accurate predictions. An exception is observed in the case of the 40 mm diameter steel store, where the second mode appears to produce a closer match. Unlike the other configurations, numerical results for the 40 mm steel store overestimate the experimentally measured frequency values.

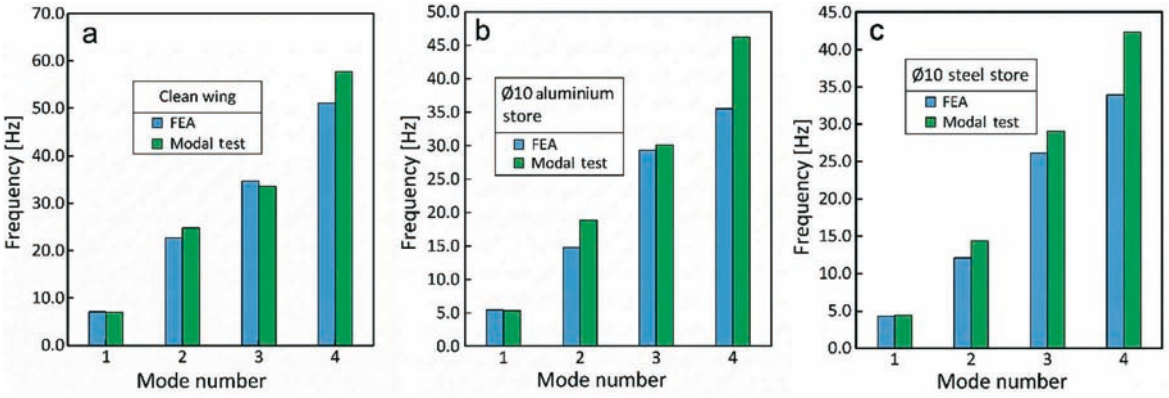

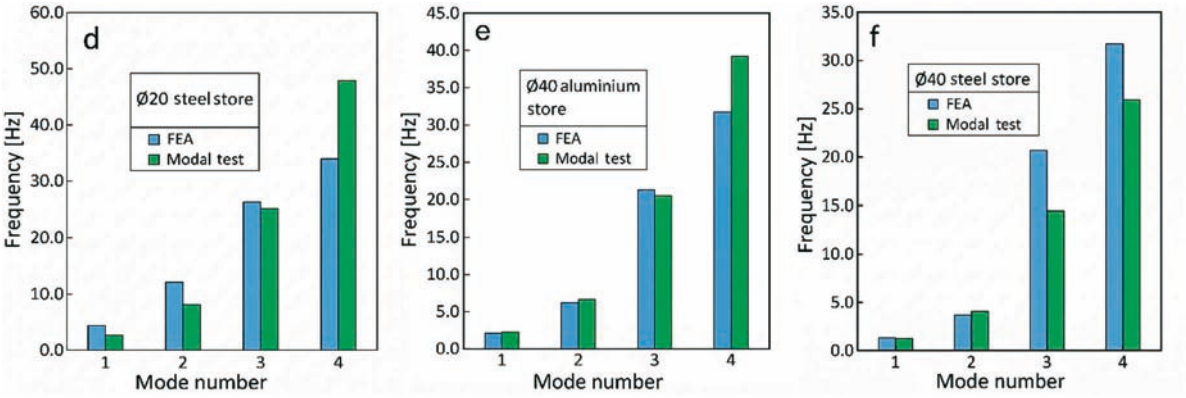

Fig. 8 FEA and GVT frequency results via mode number plot of wing plate (a) clean wing, (b) with Ø10 alum. store, (c) with Ø10 steel store, (d) with Ø20 steel store, (e) with Ø40 alum. store and (f) with Ø40 steel store

3.3 Flutter ZAERO analysis results

In this section, detailed results of the flutter analysis carried out for each external store configuration are presented. The aeroelastic model of the test specimens was constructed using ZAERO software, which provides a robust framework for simulating unsteady aerodynamic and structural interactions. The mode shape data obtained in the preceding section were incorporated into the ZAERO/ZONA6 module and served as essential input for the flutter computations. Based on the results obtained from the k-method, which aligned more closely with wind tunnel test data than the g-method, Fig. 9 presents the *V-g* and *V-f* plots corresponding to the first four vibration modes of the wing plate across different store conditions.

For the clean wing configuration, where no external mass is attached, the flutter analysis indicated that under an assumed structural damping ratio ranging from 0% to 4%, the flutter speed varied between 67.8 m/s and 74.5 m/s. In comparison, the same conditions evaluated by the g-method produced flutter speeds between 56.3 m/s and 57.4 m/s. Similarly, the flutter frequency was observed to vary between 17.7 Hz and 17.0 Hz for the k-method, while the g-method results fell between 16.0 Hz and 16.4 Hz, as detailed in Table 5. At a critical speed of 67.8 m/s, the damping ratio of the first mode was found to decline to zero, indicating the onset of flutter. This behaviour is illustrated in Figures 9a and 9b. Additionally, the analysis of output data confirmed that the modes primarily responsible for initiating flutter were the first and second structural modes.

Table 5 Flutter analysis results for clean wing and all types of store

Wing tip	Damping [G]		0%	0.5%	1.0%	1.5%	2.0%	2.5%	3.0%	3.5%	4.0%
Clean wing	g-method	*V* [m/s]	56.3	56.4	56.6	56.7	56.9	57.0	57.1	57.3	57.4
	k-method		67.8	68.6	69.5	70.3	71.1	72.0	72.8	73.6	74.5
	g-method	*f* [Hz]	16.4	16.3	16.3	16.3	16.2	16.2	16.1	16.1	16.0
	k-method		17.7	17.6	17.5	17.4	17.4	17.3	17.2	17.1	17.0
Ø10 mm aluminium store	g-method	*V* [m/s]	55.2	56.7	57.8	58.7	58.8	58.9	59.0	59.1	59.1
	k-method		67.0	67.2	67.3	67.3	67.4	67.5	67.6	67.7	67.8
	g-method	*f* [Hz]	11.1	11.0	10.8	10.7	10.6	10.6	10.5	10.5	10.5
	k-method		11.4	10.9	10.7	10.6	10.6	10.6	10.5	10.5	10.4
Ø20 mm aluminium store	g-method	*V* [m/s]	53.6	55.8	56.6	58.6	58.9	59.3	60.4	60.2	60.3
	k-method		62.9	62.9	65.9	62.9	62.9	62.9	62.9	62.9	62.9
	g-method	*f* [Hz]	31.0	30.6	30.4	30.2	30.0	7.70	7.70	7.70	7.70
	k-method		7.80	7.70	7.70	7.60	7.50	7.50	7.40	7.40	7.30

Wing tip	Damping [G]		0%	0.5%	1.0%	1.5%	2.0%	2.5%	3.0%	3.5%	4.0%
Ø40 mm aluminium store	g-method	V [m/s]	52.3	54.2	55.7	56.8	57.8	58.9	60.0	60.1	61.6
	k-method		56.4	56.6	56.7	56.9	57.0	57.2	57.3	57.5	57.6
	g-method	f [Hz]	28.5	28.2	28.0	27.9	27.7	27.6	27.4	27.4	27.3
	k-method		4.20	4.10	4.10	4.10	4.10	4.10	4.10	4.10	4.10
Ø10 mm steel store	g-method	V [m/s]	54.4	55.3	58.1	60.7	61.6	61.7	61.8	61.9	62.0
	k-method		63.8	63.0	63.0	63.0	63.1	63.1	63.1	63.1	63.2
	g-method	f [Hz]	31.4	31.0	30.7	30.5	8.50	8.50	8.50	8.50	8.50
	g-method		8.50	8.40	8.30	8.30	8.30	8.20	8.20	8.10	8.10
Ø20 mm steel store	g-method	V [m/s]	51.8	52.7	53.9	54.6	55.3	56.7	59.0	59.9	60.5
	k-method		59.4	59.5	59.6	59.7	59.8	59.9	60.0	60.1	60.1
	g-method	f [Hz]	30.0	29.7	29.5	29.3	29.1	29.0	28.8	28.7	28.6
	k-method		5.00	5.00	5.00	5.00	4.90	4.90	4.90	4.90	4.90
Ø40 mm steel store	g-method	V [m/s]	49.5	50.2	50.9	52.6	54.3	55.7	57.0	58.2	59.4
	k-method		54.0	54.2	54.4	54.6	54.8	55.1	55.3	55.5	55.7
	g-method	f [Hz]	28.1	27.9	27.8	27.6	27.4	27.3	27.2	27.1	27.0
	k-method		2.60	2.60	2.60	2.60	2.60	2.60	2.60	2.60	2.60

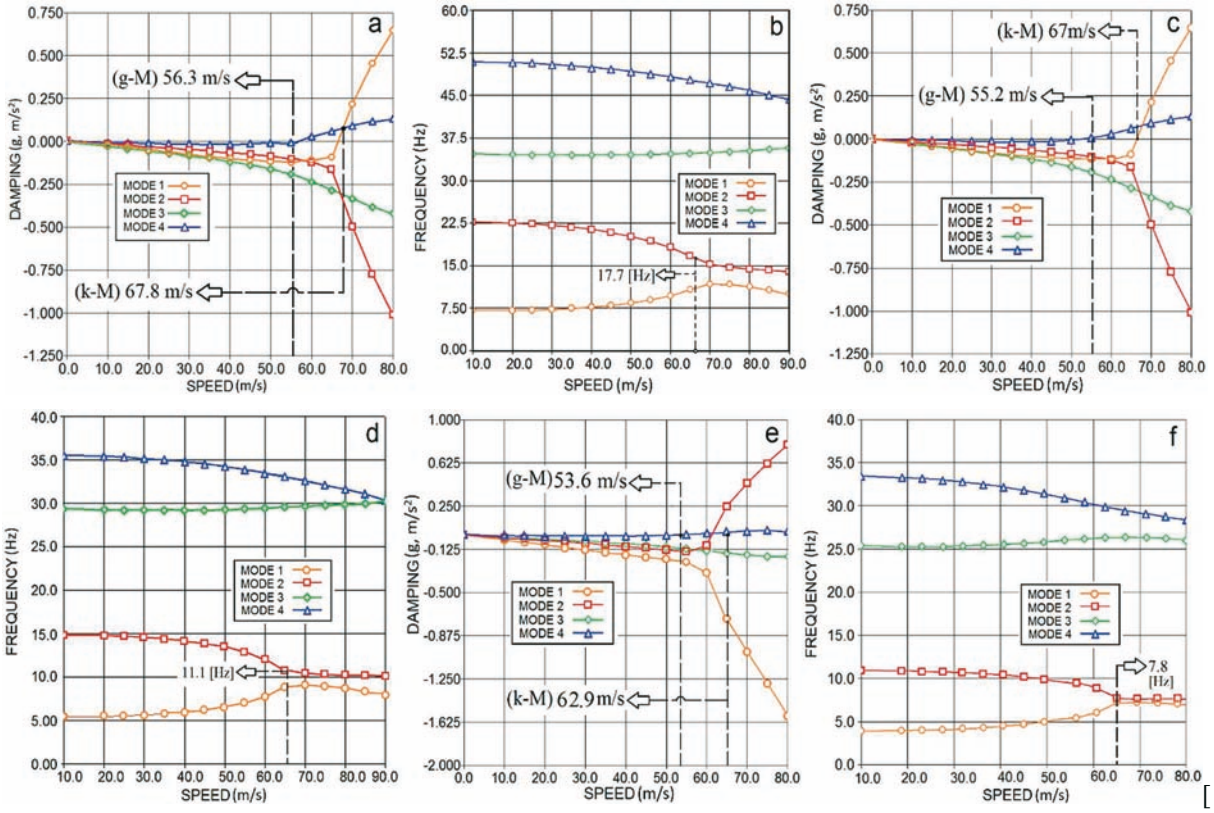

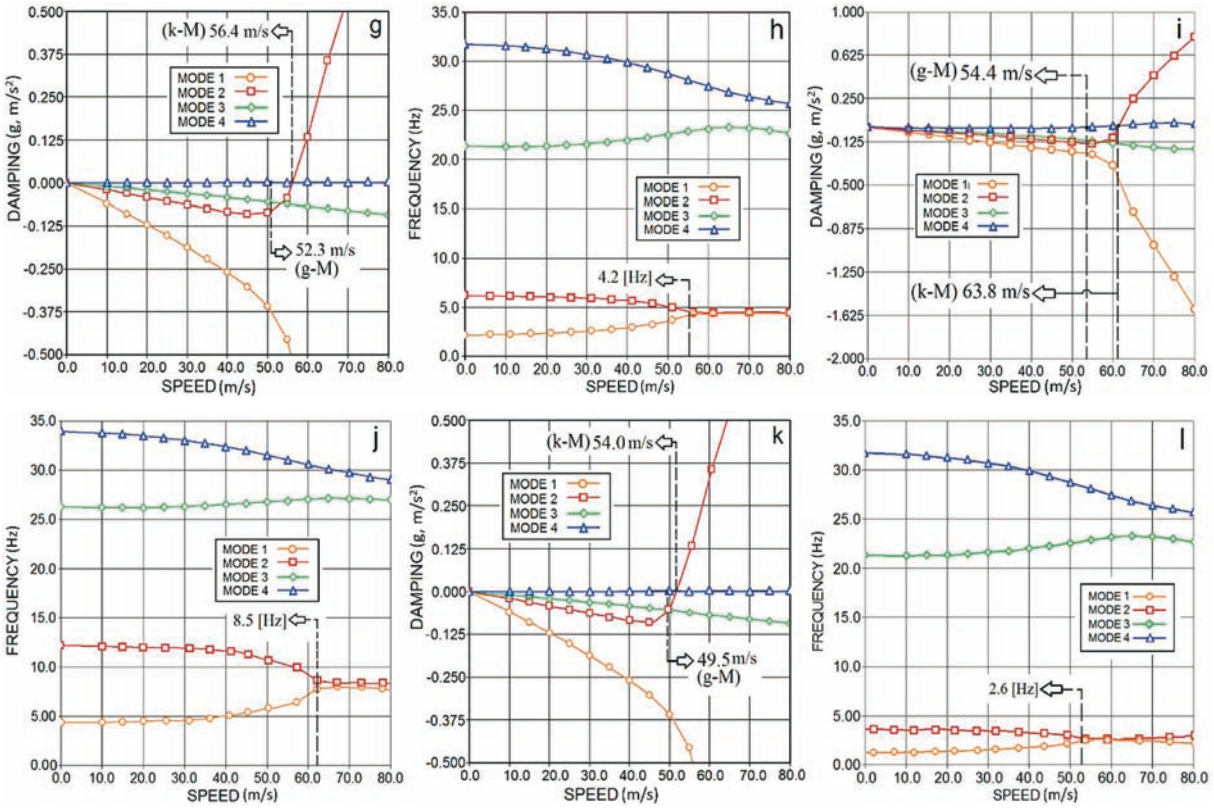

Fig. 9 *V-g* and *V-f* plot of wing plate (a)-(b) clean wing, (c)-(d) with Ø10 aluminium store, (e)-(f) with Ø20 aluminium store, (g)-(h) with Ø40 aluminium store, (i)-(j) with Ø10 steel store, and (k)-(l) with Ø40 steel store

For the steel store with the largest diameter and mass (40 mm), the modal analysis results obtained using the second mode shape indicate a flutter speed of 54.0 m/s and a flutter frequency of 2.60 Hz, as illustrated in Fig. 9k and Fig. 9l. At a velocity of 54.0 m/s, the damping of the second mode drops to zero, which marks the onset of flutter for this configuration. According to the data extracted from the output file, the first four modes contribute to the onset of flutter. Referring to the wind tunnel results presented in Table 5, it is observed that as the mass of the external store attached to the wing increases, the system reaches the flutter condition at lower speeds. When examining the results in terms of flutter frequency, it is evident that increasing the mass of the underwing external store causes a decrease in flutter frequency, as shown in Fig. 10a. In terms of both flutter frequency and flutter speed, the results obtained using the k-method are closer to the experimental data compared to those obtained using the g-method. Furthermore, the flutter speeds predicted by both the k-method and the g-method exhibit a trend that is consistent with the wind tunnel data. In other words, the flutter speed decreases as the external store mass increases, as can be seen in Fig. 10b.

For flutter frequency, the ZAERO analysis results are on average 15% lower than the wind tunnel test results; this discrepancy increases up to 25% depending on the speed values. In Figure 11, the comparison of flutter speed and frequency is presented with respect to the g-method, k-method, and the experimental results, respectively, according to the method used. These comparisons are provided to examine the effect of store diameter, i.e., the influence of geometric properties.

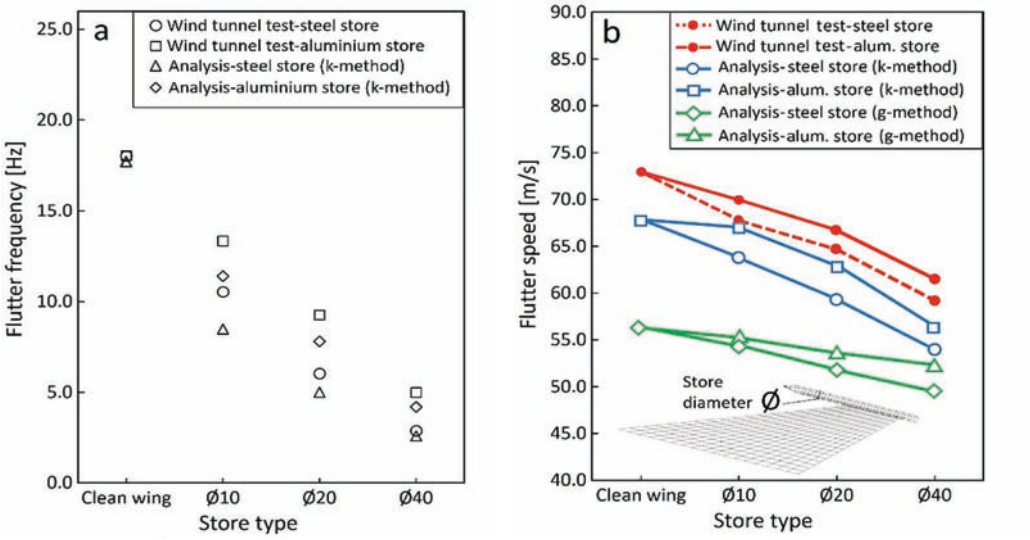

Fig. 10 Comparison of (a) flutter frequency (b) flutter speed via store type for all methods

When examining the frequencies, it is observed that the g-method exhibits significantly larger deviations compared to the k-method as the store mass increases (as seen in Fig. 11a). Therefore, the current system can be estimated with higher accuracy using the k-method. As illustrated in Fig. 11b, the flutter speed predictions from the k-method also align more closely with the experimental results. Hence, under the boundary conditions defined in this study, the g-method does not provide reliable results for predicting flutter speeds. When considering flutter frequency predictions under identical loading conditions, the k-method results differ from the wind tunnel test data by approximately 0.3 to 2 Hz. This discrepancy corresponds to a variation of about 3 to 5 m/s in flutter speeds. In cases where the store masses are relatively close (e.g., clean wing vs. Ø10 aluminium store, and Ø10 steel vs. Ø20 aluminium store), the frequency and speed values appear quite similar. However, as the store mass increases, noticeable differences emerge in both flutter frequency and speed. For instance, the Ø40 steel store, which is approximately five times heavier than the Ø10 aluminium store, results in a flutter speed that is about 6 m/s lower. This change corresponds to a frequency difference of roughly 5.5 Hz. The variation in flutter parameters with respect to store mass is presented in Fig. 12a as the frequency-mass relationship, and in Fig. 12b as the speed-mass relationship.

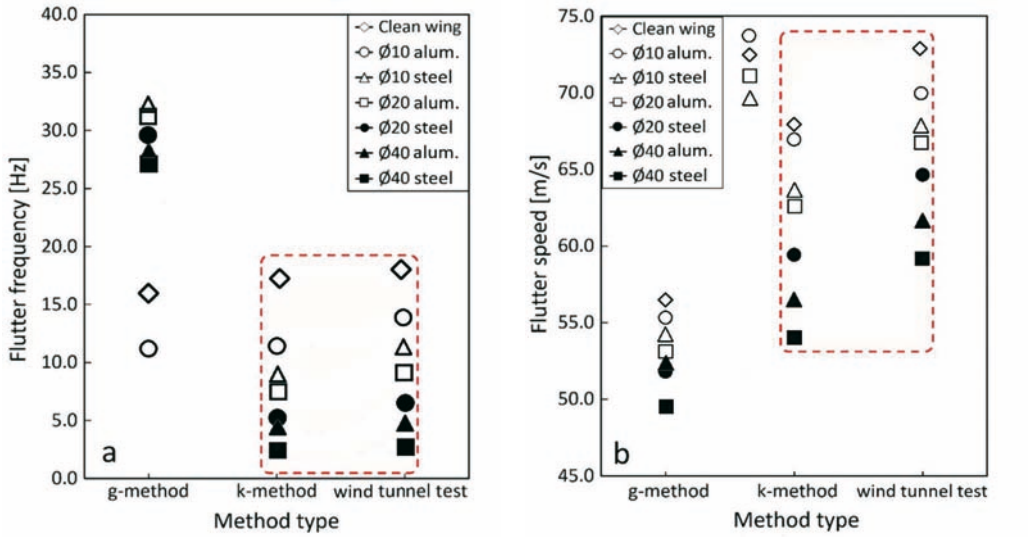

Fig. 11 Comparison of (a) flutter frequency and (b) speed vs. store diameter

Regarding the g-method frequency predictions, it is evident that at lower store masses, the g-method, k-method, and wind tunnel results are in close agreement as shown in Fig. 12a.

However, after the 224 g threshold (Ø20 aluminium store), the g-method frequency shows a disproportionately large, nearly threefold increase. Additionally, in terms of flutter speed, the g-method results remain approximately 10 m/s lower than those obtained from the k-method and wind tunnel tests (Fig. 12b). With regard to frequency, similar trends are observed across all three methods. Despite differences in aerodynamic characteristics, the flutter frequencies and speeds of low-mass configurations, such as the clean wing and the 70 g Ø10 aluminium store, are quite close. On the other hand, as the store mass increases, the flutter parameters begin to diverge significantly, as shown in both Fig. 12a and Fig. 12b. Janardhan and Grandhi [15] reported similar findings in their study involving underwing-tip stores with structural non-mass (NSM) values twice and three times higher than the base configuration. For low supersonic and transonic flow conditions, they observed that the flutter speed dropped from 950 knots (clean wing) to 700 knots when the NSM was tripled at 0.4 Mach.

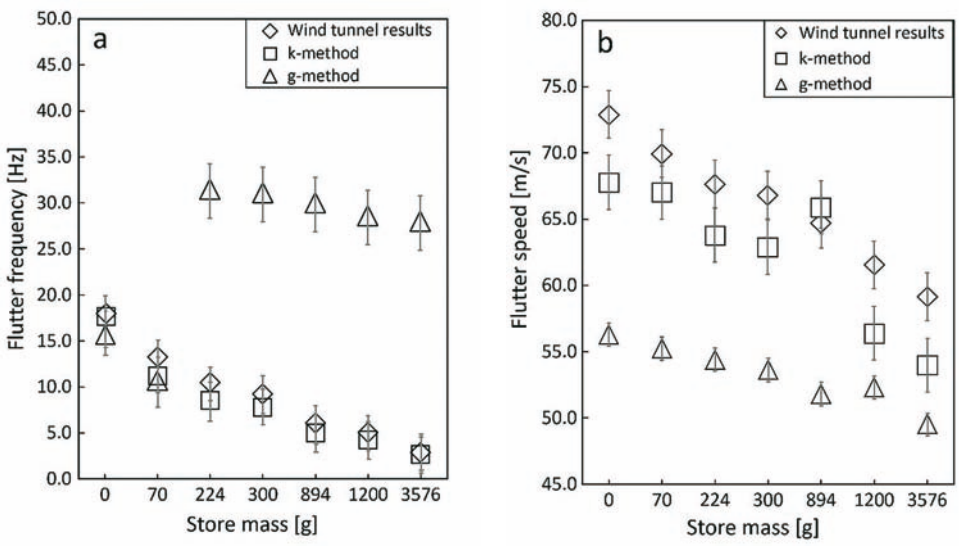

Fig. 12 A comparison of (a) flutter frequency and (b) speed vs. the store mass

The store-type comparison in Fig. 13 further reinforces these trends. For geometrically identical stores, increasing the material density from aluminium to steel consistently shifts both flutter frequency and speed to lower values. Flutter frequency responds more strongly to added tip mass than flutter speed, suggesting that inertial coupling at the wing tip dominates aeroelastic behaviour under the subsonic conditions examined here. The store type therefore offers a practical means of isolating inertial effects from aerodynamic ones, reinforcing the validity of the flat-plate modelling approach adopted in this study.

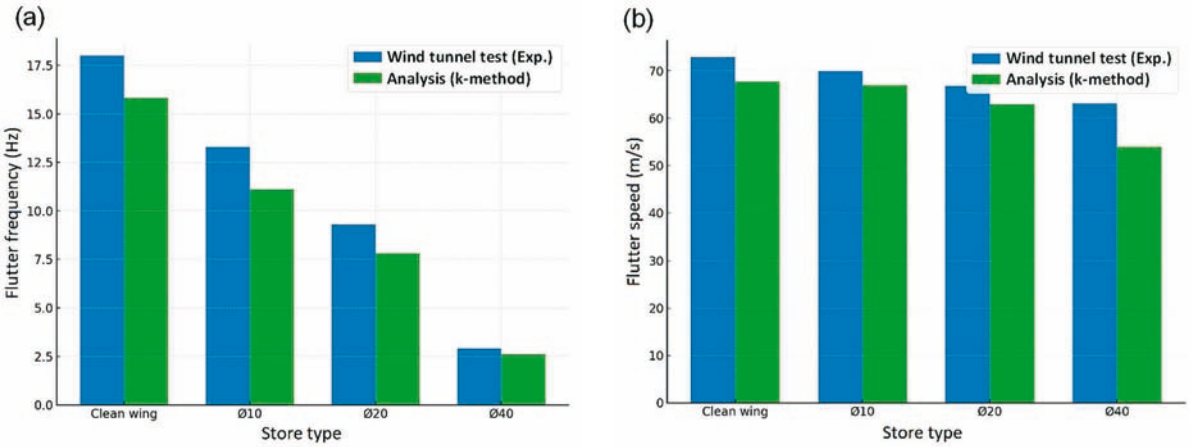

Fig. 13 Comparison of (a) flutter frequency and (b) speed vs. store type

Based on the findings obtained, the strong correlation between the k-method predictions and the wind tunnel measurements, as clearly demonstrated in Fig. 11a–b, confirms the suitability of this approach for reliable flutter estimation in low-speed subsonic conditions. These results indicate that, for the tip-store configurations and boundary conditions examined in this study, the k-method can be confidently employed to predict both flutter frequency and flutter speed without requiring additional experimental validation, provided that the same structural and aerodynamic constraints are strictly maintained (see Fig. 13). Furthermore, a noticeable and consistent decrease in flutter frequency was observed when external stores with masses significantly higher than the clean-wing mass of 754 g were attached. This effect became particularly evident for the Ø40 aluminium (1200 g) and Ø40 steel (3576 g) configurations, where the added mass substantially increased the inertial loading on the wing. For instance, the flutter frequency, measured as approximately 18 Hz for the clean-wing case, dropped markedly to around 2.69 Hz in the presence of the Ø40 steel store, as illustrated in Fig. 13a, highlighting the pronounced sensitivity of aeroelastic stability to tip-mounted mass variations.

While the present analysis adopts a simplified flat-plate representation of the F-16 wing, this modelling strategy was intentionally used to isolate the structural and inertial effects of varying store masses. Aligned with this intent, Turner [11] showed that a simplified wing/store representation can still reveal inertia-driven shifts in flutter characteristics without being dominated by detailed store aerodynamics. Maxwell et al. [38] similarly demonstrated that ZAERO/ZONA-based analyses can retain the dominant unsteady-aerodynamic mechanisms governing flutter trends even with reduced geometric fidelity. Golparvar et al. [41] supported this perspective experimentally by extracting the main aeroelastic trends from simplified store-equipped configurations. Accordingly, the results here should be interpreted as reliable estimates of relative, mass-induced changes in flutter speed and frequency under consistent boundary conditions, rather than absolute flutter limits for the full aircraft.

4. Conclusions

The external stores mounted beneath the wing significantly influence the dynamic aeroelastic stability of the structure from both structural and aerodynamic perspectives. It has been observed that stores attached to the under-wing reduce the natural frequencies due to their inertial effects and lower the flutter speed depending on their mass. For all tested wing configurations, the initial modal analysis results exhibited closer agreement with Ground Vibration Test (GVT) outcomes, emphasising the importance of validating numerical modal analyses through experimental testing prior to flutter simulations. With respect to flutter frequency, the ZAERO®/k-method predictions showed better agreement with wind tunnel measurements compared to the g-method. Both numerical and experimental findings consistently revealed that increasing the store mass leads to a reduction in both flutter frequency and flutter speed. However, while flutter frequency decreases nearly proportionally with added mass, the reduction in flutter speed is less pronounced. This indicates that store mass has a more dominant effect on flutter frequency than on flutter speed. The results confirm that the k-method provides a reliable means of estimating flutter parameters for the examined under-wing and tip store configurations and boundary conditions. This method offers an effective alternative for flutter prediction in subsonic regimes, potentially reducing the need for extensive experimental testing. Additionally, under low-speed subsonic conditions, the impact of store mass on flutter behaviour is found to be more significant than the aerodynamic characteristics of the store itself.

REFERENCES

[1] Lanchester, FW. “Torsional vibration of the tail of an aeroplane”, Aeronaut Research Com R & M. 276, part I (1916).

[2] Bairstow, L.; Fage, A.: “Oscillations of the tail plane and body of an aeroplane in flight”, Aeronaut Research Com R&M 276, part ii (1916).

[3] Blasius, H.: Über schwingung serscheinungen an einholmigen unter flügeln. Zeitschrift für Flugtechnik und Motorluftschiffahrt, 16, 39-42 (1925).

[4] Smilg, B.: The Instability of Pitching Oscillations of an Airfoil in Subsonic Incompressible Potential Flow. J Aeronaut Sci 16, 691-696 (1949). https://doi.org/10.2514/8.11885

[5] Cheilik, H.; Frissel, H.: "Theoretical criteria for Single degree of freedom flutter at supersonic speeds", Cornell Aeronaut Lab Rept CAL-7A (1947).

[6] Cunningham, H.J.: "Analysis of pure-bending flutter of a cantilever swept wing and its relation to bending-torsion flutter", NACA Tech Note 2461 (1951).

[7] Greidanus, J.H.: Low-speed flutter. J Aeronaut Sci 16, 127-128 (1949).

[8] Dugundji, J.: Theoretical consideration of panel flutter at high supersonic Mach No. AIAA J 4(7), 1257-1266 (1966). https://doi.org/10.2514/3.3657

[9] Dowell, E.H.: Nonlinear oscillation of a fluttering plate. AIAA J 4(7), 1267-1288 (1966). https://doi.org/10.2514/3.3658

[10] Kosmatka, J.B.: Flexure-torsion behavior of prismatic beam. AIAA J 31(1), 170-179 (1993). https://doi.org/10.2514/3.11334

[11] Turner, C.D.: Effect of store aerodynamics on wing/store flutter. J Aircraft 19(7), 574-580 (1981). https://doi.org/10.2514/3.57431

[12] Fazelzadeh, S.A.; Mazidi, A.; Rahmati, A.R.; Marzocca, P.: The effect of multiple stores arrangement on flutter speed of a shear deformable wing subjected to pull-up angular velocity. Aeronautical J 113(1148), 661-668 (2009). https://doi.org/10.1017/S0001924000003328

[13] Farhat, C.; Chiu, E.K.; Amsallem, D.; Schotte, J.S.; Ohayon, R.: On the modeling of fuel sloshing and its physical effects on flutter. AIAA J 51(9), 2252-2265 (2013). https://doi.org/10.2514/1.J052299

[14] Jun, S.; Tischler V.A.; Venkayya V.B.: Multidisciplinary design optimization of a built-up wing structure with tip missile. J Aircraft 40(6), 1093-1098 (2003). https://doi.org/10.2514/2.7219

[15] Janardhan, S.; Grandhi, R.V.; Eastep, F.; Sanders, B.: Parametric studies of transonic aeroelastic effects of an aircraft wing/tip store. J Aircraft 42(1), 253-263 (2005). https://doi.org/10.2514/1.627

[16] Librescu, L; Song, O.: Dynamics of composite aircraft wings carrying external stores. AIAA J 46(3), 568-577 (2008). https://doi.org/10.2514/1.25541

[17] Currao, G.M.D.: Transonic leading-edge stall flutter: modelling, simulations and experiments. J Fluid Mech 984, A54 (2024). https://doi.org/10.1017/jfm.2024.238

[18] Goizueta, N.; Wynn, A.; Palacios, R.; Drachinsky, A.; Raveh, D.E.: Flutter predictions for very flexible wing wind tunnel test. AIAA 2021 SciTech Forum, Virtual event, 11-15 & 19-21 January 2021. https://doi.org/10.2514/1.C036710

[19] Kim, C.; Ji, C.; Bang, J.; Koh, G.; Choi, N.: A survey on structural coupling design and testing of the flexible military aircraft. Int J Aeronaut Space Sci 25, 122–145 (2024). https://doi.org/10.1007/s42405-023-00643-y

[20] Kim, C.; Ji, C.; Koh, G.; Choi, N.: Review on flight control law technologies of fighter jets for flying qualities. J Aeronaut Space Sci 24, 209–236 (2023). https://doi.org/10.1007/s42405-022-00560-6

[21] Healy, F.; Courcy, J.D.; Gu, H.; Rezgui, D.; Cooper, J.; Wilson, T.; Castrichini, A.: On the dynamic behavior of wings incorporating floating wingtip fuel tanks. J Aircraft 61(3), 1-38 (2023). https://doi.org/10.2514/1.C037519

[22] Yu, Q.; Damodaran, M.; Khoo, B.C.: Predicting wing-pylon-nacelle configuration flutter characteristics using adaptive continuation method. Adv Aerodyn 5, 21, (2023). https://doi.org/10.1186/s42774-023-00152-2

[23] Basiri, M.; Farrokhfal, H.; Mosayebi, M.; Koohi, R.: Rapid flutter analysis for low-aspect-ratio wings with a control surface. J Appl Mech Tech Phys 63(1), 59-66 (2022). https://doi.org/10.1134/S0021894422010102

[24] Balakrishnan, A.V.; Tuffaha, A.M.; Patino, I.; Melnikov, O.: Flutter analysis of an articulated high aspect ratio wing in subsonic airflow. J Frank Inst 351, 4230–4250 (2014). https://doi.org/10.1016/j.jfranklin.2014.04.010

[25] Bantschef, K.; Breitsamter, C.: Design and investigation of an aeroelastically scaled delta-wing wind tunnel model for dynamic load analysis. CEAS Aeronaut J 16, 275–291 (2025). https://doi.org/10.1007/s13272-024-00795-x

[26] Guo, H.; Yan, Y.; Xia, H.; Yu, L.; Lv, B.: The Prediction and Correction Method of Aircraft Static Aeroelastic Effects: A Review of Recent Progress. Actuators 11, 309 (2022). https://doi.org/10.3390/act11110309

[27] Dinulovic, M.; Benign, A.; Rasuo, B.: Composite fins subsonic flutter prediction based on machine learning. Aerospace 11, 26 (2024). https://doi.org/10.3390/aerospace11010026

[28] Chen, P.C.; Sulaeman, E.; Liu, D.D.; Denegri Jr., C.M.: "Influence of external store aerodynamics on flutter/LCO of a fighter aircraft", 43rd AIAA/ASME/ASCE/AHS/ASC Structures, Structural Dynamics, and Materials Conference, Denver, Colorado, USA (22-25 April 2002). https://doi.org/10.2514/6.2002-1410

[29] Lee, D.H.; Chen, P.C.: "Studies of aerodynamic influence of under-wing stores on flutter characteristics of F-16", 50th AIAA/ASME/ASCE/AHS/ASC Structures, Structural Dynamics, and Materials Conference, Palm Springs, California, USA (4-7 May 2009). https://doi.org/10.2514/6.2009-2463

[30] ZONA Tech. Inc., "ZAERO V8.5 Theoretical Manual", 21st Edition, June 2011.

[31] Tang, D.; Dowell, E.H.: Experimental aeroelastic models design and wind tunnel testing for correlation with new theory. Aerospace 3(2), 12 (2016). https://doi.org/10.3390/aerospace3020012

[32] Gern, F.H.; Librescu, L.: Static and dynamic aeroelasticity of advanced aircraft wings carrying external stores. AIAA J 36(7), 1121-1129 (1998). https://doi.org/10.2514/2.499

[33] Yaman, K.: Subsonic flutter of cantilever rectangular PC plate structure. Int J Aerospace Eng 2016, 1-10 (2016). https://doi.org/10.1155/2016/9212364

[34] Chen, P.C.: Damping Perturbation Method for Flutter Solution: The g-Method. AIAA J 38(9), 1519-1527 (2000). https://doi.org/10.2514/2.1171

[35] Pollock, S.J.; Sotomayer, W.A.; Hutsel, L.J.; Coley, D.E.: Evaluation of methods for prediction and prevention of wing/store flutter. J Aircraft 19(6), 492-498 (1981). https://doi.org/10.2514/3.57419

[36] Bennani, S.; Beuker, B.; Staveren, J.W.; Meijer, J.J.: Flutter Analysis for the F-16A/B in Heavy Store Configuration. J Aircraft 42(6),1566-1575 (2005). https://doi.org/10.2514/1.7339

[37] Santos, L.C.; Silva, R.G.A.; Castro, B.M.; Marto, A.G.; Alonso, A.C.P.: "Modeling the subsonic aerodynamics of aircraft with external stores for flutter analysis", Proceedings of the 10th Brazilian Congress of Thermal Sciences and Engineering, ENCIT 2004. ABCM, Rio de Janeiro, Brazil, Nov. 29-Dec. 03, (2004).

[38] Maxwell, D.L.; Denegri, Jr. C.M.; Dawson, K.S.; Dubben, J.: "Effect of Underwing Store Aerodynamics on Analytically Predicted F-16 Aeroelastic Instability", 48th AIAA/ASME/ASCE/AHS/ASC Structures, Structural Dynamics, and Materials Conference, 23-26 April 2007, Honolulu, Hawaii, USA (2007). https://doi.org/10.2514/6.2007-2366

[39] Heinze, S.; Ringertz, U.; Borglund, D.: Assessment of uncertain external store aerodynamics using μ-p flutter analysis. J Aircraft 46(3), 1062-1067 (2009). https://doi.org/10.2514/1.39158

[40] Cui, P.; Han, J.: Prediction of flutter characteristics for a transport wing with wingtip devices. Aerosp Sci Technol 23, 461–468 (2012). https://doi.org/10.1016/j.ast.2011.10.005

[41] Golparvar, H.; Irani, S.; Mousavi Sani, M.: Experimental investigation of linear and nonlinear aeroelastic behavior of a cropped delta wing with store in low subsonic flow. J Braz Soc Mech Sci Eng 38, 1113–1130 (2016).https://doi.org/10.1007/s40430-015-0436-z

[42] Gilioli, A.; Manes, A.; Ringertz, U.; Giglio, M.: Investigation about the structural nonlinearities of an aircraft pylon. J Aircraft 56(1), 1-11 (2018). https://doi.org/10.2514/1.C034882

[43] Yuan, W.; Zhang, X.: Numerical Stabilization for Flutter Analysis Procedure. Aerospace 10, 302 (2023). https://doi.org/10.3390/aerospace10030302

[44] Kariv, D.; Kunz, D.L.; Lovnovich, M.: Toward an efficient method for F-16 limit cycle oscillation prediction. J Aircraft 61(2), 558-569 (2024). https://doi.org/10.2514/1.C037391

[45] Göge, D.; Böswald, M.; Füllekrug, U.; Lubrina, P.: Ground vibration testing of large aircraft – state-of-the-art and future perspectives. LMS Conference Europe, Stuttgart, Germany (April 17-18, 2007).

Submitted: 20.06.2025

Accepted: 02.02.2026

Kemal Yaman*
OSTİM Technical University, Industrial Design Department, 06374, Ankara, Turkey

Mevlüt Burak Dalmış
Defense Industries Research and Development Institute, Turkish Scientific and Technical Research Council, 06261, Ankara, Turkey

*Corresponding author:
kemal.yaman@ostimteknik.edu.tr